Hydrogen oxidation mechanisms on Ni/yttria stabilized zirconia anodes: Separation of reaction pathways by geometry variation of pattern electrodes

M.C. Doppler[a,b], J. Fleig[b], M. Bram[a,c], A.K. Opitz[a,b,*]

[a] *Christian Doppler Laboratory for Interfaces in Metal-Supported Electrochemical Energy Converters, Getreidemarkt 9/164-EC, 1060 Wien, Austria*
[b] *Institute of Chemical Technologies and Analytics, TU Wien, Getreidemarkt 9-164/EC, 1060 Vienna, Austria*
[c] *Institute of Energy Research (IEK-1) Forschungszentrum Jülich, Wilhelm-Johnen-Straße, D-52425 Jülich, Germany*

HIGHLIGHTS

- Long term stable pattern anodes were prepared.
- Geometry variation allows separation of hydrogen oxidation pathways.
- Novel hydrogen oxidation pathway scaling with electrode area was identified.
- Area pathway explains current discrepancies existing in literature.

ARTICLE INFO

ABSTRACT

Nickel/yttria stabilized zirconia (YSZ) electrodes are affecting the overall performance of solid oxide fuel cells (SOFCs) in general and strongly contribute to the cell resistance in case of novel metal supported SOFCs in particular. The electrochemical fuel conversion mechanisms in these electrodes are, however, still only partly understood. In this study, micro-structured Ni thin film electrodes on YSZ with 15 different geometries are utilized to investigate reaction pathways for the hydrogen electro-oxidation at Ni/YSZ anodes. From electrodes with constant area but varying triple phase boundary (TPB) length a contribution to the electro-catalytic activity is found that does not depend on the TPB length. This additional activity could clearly be attributed to a yet unknown reaction pathway scaling with the electrode area. It is shown that this area related pathway has significantly different electrochemical behavior compared to the TPB pathway regarding its thermal activation, sulfur poisoning behavior, and H_2/H_2O partial pressure dependence. Moreover, possible reaction mechanisms of this reaction pathway are discussed, identifying either a pathway based on hydrogen diffusion through Ni with water release at the TPB or a path with oxygen diffusion through Ni to be a very likely explanation for the experimental results.

1. Introduction

As global energy demand is expected to further increase in the future and emission of carbon dioxide is aimed to be reduced, novel and efficient energy conversion technologies are urgently required [1]. Solid oxide fuel cells (SOFCs) are compatible with a variety of possible future fuel infrastructures (e.g. hydrogen, or hydrocarbons synthesized from renewable resources) as they are capable of high chemical-to-electrical energy conversion efficiencies for a diverse set of fuels. State-of-the-art SOFCs utilize nickel/yttria stabilized zirconia (YSZ) cermet anodes on the fuel side, which usually perform well but under certain conditions may contribute significantly to the overall internal losses in the fuel cell, especially when operating with sulfur containing fuels. Moreover, in case of metal supported SOFCs the microstructure of the Ni/YSZ anode is usually less ideal than in electrolyte or anode supported systems. This is due to the fact that the anode sintering step during SOFC production is performed under reducing conditions facilitating Ni grain growth and thus increasing the anode polarization resistance [2,3].

Despite the importance of the anode for the efficiency of the overall SOFC system, the reaction mechanism of the most basic fuel reaction – the hydrogen oxidation – is still not very well understood [4–20]. On an

oxide ion conducting electrolyte the electrochemical hydrogen oxidation at the anode can be written in Kröger-Vink notation as follows:

$$H_2 + O_O^{\times} \rightleftarrows H_2O + V_O^{\bullet\bullet} + 2\ e' \tag{1}$$

In-depth understanding of mechanistic aspects, such as individual elementary steps of equation (1), are difficult to explore using commercial cermet anodes, particularly due to transport phenomena of ions, electrons and gaseous species within the porous network of a cermet anode contributing to the entire electrode polarization. This is why a number of previous studies dealing with hydrogen oxidation in Ni/YSZ electrodes utilized micro-patterned thin film Ni electrodes [4,6,12,15,20]. Besides usually avoiding problems arising from transport limitations, pattern electrodes also offer the opportunity of deliberate variation of the electrode geometry. Based on such geometry variations, these previous publications reported the rate limiting step of the hydrogen oxidation to be located at the triple phase boundary (TPB) between Ni, YSZ and the gas phase. In particular, this conclusion was obtained by measuring the polarization resistance of electrodes with varying TPB lengths and determining the exponent α of the following equation:

$$R_{Pol} = R_{Pol,0} \cdot l_{TPB}^{-\alpha} \tag{2}$$

In case the rate limiting step of the reaction is located at the triple phase boundary a value of 1 should be obtained for the exponent α. Measured values of α include 0.8 ± 0.04 [6], 0.67–1.2 [7], and 0.7–0.72 [20], thus significantly deviating from the expected α = 1. Moreover, also Refs. [4,21] noted deviations from proportionality between the inverse polarization resistance and the TPB length. As the aforementioned values of α are based on linear regression with very few data points, a more in-depth analysis of the published data is hardly possible. Consequently, a clear and unambiguous investigation of electrochemical pathways of H_2 oxidation on Ni/YSZ anodes is still lacking. For a knowledge-based optimization of anodes for metal supported SOFCs, as well as for a purposive increase of their sulfur tolerance, a more detailed understanding of the electrochemical hydrogen oxidation is needed.

In this contribution the deviations of the experimental data from the simple mechanistic picture of a solely TPB-active Ni anode are revisited by a detailed investigation of a large number of micro-patterned thin film Ni-electrodes employing different geometries at different temperatures and in different gas atmospheres containing H_2, H_2O and H_2S. In particular, numerous complex-shaped Ni thin film electrodes with different TPB lengths but nominally identical areas (and vice versa) were fabricated and electrochemically characterized at SOFC operation temperatures by impedance spectroscopy. On the basis of this data set, deviations from a simple geometrical relation between polarization resistance and TPB length could be clearly confirmed, which is supported by a detailed statistical analysis of the electrochemical results. Moreover, the deviation from a simple proportional relationship between TPB length and inverse polarization resistance is critically discussed in terms of an additional electrochemical H_2 oxidation pathway, which scales with the area of the Ni electrode and exists in parallel to the 'classical' TPB-path. The electrochemical properties of the two pathways are characterized in terms of their temperature dependence, sulfur poisoning behavior, as well as p_{H2} and p_{H2O} dependence. Based on these findings two possible reaction mechanisms are proposed for the area related pathway and possible connections with the TPB path are suggested. Discovery of the additional area-related H_2 oxidation pathway on Ni anodes thus further advances the understanding of the hydrogen oxidation at Ni/YSZ electro-catalysts and may serve as a basis for a knowledge-based optimization of SOFC cermet anodes.

2. Experimental

Micro-structured nickel thin film electrodes with a nominal film
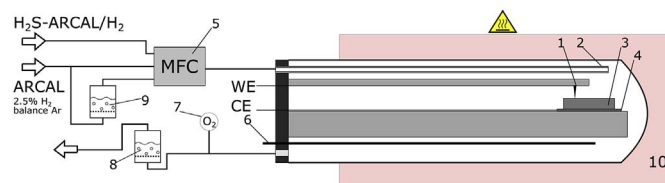

Fig. 1. Schematic drawing of the measurement setup. 1 Contacting needle (Ni), 2 Gas inlet, 3 sample, 4 counter electrode contact, 5 mass flow controller, 6 thermocouple, 7 lambda probe, 8 H_2S scrubber, 9 humidifier, 10 furnace.

thickness of 1200 nm were prepared on (111)-oriented YSZ single crystals (Crystec, Germany) with pre-sintered NiO/YSZ counter electrodes by magnetron sputtering, photolithographic structuring, and chemical etching. The individual microelectrodes were then contacted by Ni tips and electrochemically characterized by impedance spectroscopy (Alpha A High Performance Frequency Analyzer, Novocontrol, Germany) in a homogeneously heated alumina reactor as depicted in Fig. 1. Four independent contacting tips were used to sequentially investigate four different microelectrodes in a single measurement run, for example at a constant temperature within a temperature sweep. This larger amount of measured microelectrodes significantly increases sample statistics. Impedance measurements were performed between 650 °C and 800 °C in different gas atmospheres, ranging from 2.5 kPa to 92 kPa H_2 and 0.15 kPa - 1.5 kPa H_2O. Further details on sample preparation and measurement procedure have already been published in previous work [19,22].

All electrode geometries used are sketched in Fig. 2a while an optical micrograph and a scanning electron microscopy image of typical micro-patterned electrodes are shown in Fig. 2b and c, respectively. The exact sizes of all electrodes were determined by evaluation of microscopic images in a custom program; the results are discussed below. Altogether, 59 different electrodes with 15 different sizes or shapes were investigated.

The structural stability of electrodes under measurement conditions can be seen in comparing Fig. 2a and b. After over 700 h at standard measurement conditions no significant deviations in electrode structure like pore formation could be found.

3. Results

3.1. Analysis of the electrode geometries

In the electrode series with nominally constant area but varying circumference, area related effects are expected to be ideally constant
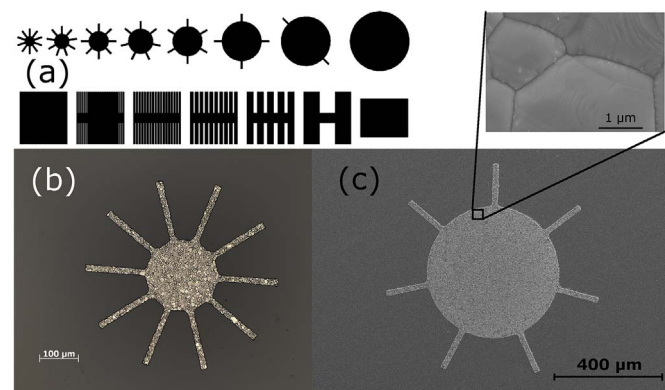

Fig. 2. (a) Depiction of the used electrode geometries on the lithographic mask. Up: Electrodes with nominally constant circumference/TPB length (decreasing circle size with compensation spikes). Down: Electrodes with nominally constant area (top and bottom areas are split into finger). (b) Reflected light microscopic image of a typical electrode after 720 h at 800 °C in H2.5W10 (2.5 kPa H_2, 0.15 kPa H_2O, balance Ar). (c) Electron microscopic image of a typical electrode with a higher magnification image at the top.